Integrated Thermal-Uniformity and Operating-Point Ranking of a Rear-Finned Monocrystalline Photovoltaic Module under Outdoor Irradiance

Hyman Norman Abramson[1,*]

[1] Retired Executive Vice President Southwest Research Institute
* Correspondence: nabramson@swri.edu

Abstract: Field cooling of photovoltaics typically entails a sole thermal or electrical effect evaluation, even though rear heat sink becomes beneficial when lowering module temperatures, improving their uniformity, and retaining their current-voltage point simultaneously. In this study, the question is investigated about the preference of a truncated multi-level fin heat sink over other rear structures of PV modules in case when temperature effectiveness, thermal uniformity, and electrical parameters are considered as a coupled decision problem. The comparative analysis is based on an outdoor data set of two monocrystalline photovoltaics having the same nominal power (120 Wp). One is a reference module without any additional features; the second module is equipped with an aluminum extrusion multi-level fin heat sink on the rear surface. Ten criterion measures include cooling effectiveness, three irradiance-dependent uniformity criteria, short circuit current, open circuit voltage, maximum power current, maximum power voltage, maximum power value, and fill factor. Grey Relational Analysis is employed to convert all heterogenic measures into criterion coefficients and integrated grade values. Sensitivity of ranking to changes of distinguishing-coefficient and weighting values is estimated in four different scenarios: thermal-only, electrical-only, domain-balanced and distinguishing-coefficient. The finned module offers 8.45 °C maximum effectiveness coefficient, higher uniformity index value at 520 W/m^2, 940 W/m^2, and 640 W/m^2, improved open circuit voltage by 1.4 V, maximum power by 9.38 W and fill factor by 0.06. Short circuit current is the sole disadvantage of a fin structure, being slightly greater than that of the reference module. Under equal criterion weights and $\zeta = 0.5$, the grey relation grade values are 0.933 and 0.400 for the finned and reference module, respectively. The order does not change in any other sensitivity scenario. The results provide a clear answer to the posed question: a truncated multi-level fin is the superior configuration as far as thermal and electrical performance are concerned.

Keywords: photovoltaic cooling; multi-level fin heat sink; temperature uniformity; outdoor photovoltaic testing; grey relational analysis; passive thermal management; current–voltage performance

Citation: Abramson, H. N. 2022. Integrated Thermal-Uniformity and Operating-Point Ranking of a Rear-Finned Monocrystalline Photovoltaic Module under Outdoor Irradiance. *TK Techforum Journal (ThyssenKrupp Techforum)* 2022(2): 79–96.

Received: June-09-2022
Accepted: September-03-2022
Published: September-30-2022

1. Introduction

Photovoltaic electricity has become the core component of renewable energy due to the possibility of rapid implementation at utility, commercial, residential, and BIPV scales. The output of any photovoltaic module, though, is affected not only by the resource of incident radiation and the module capacity indicated on its nameplate. An outdoor module has a temperature that is greater than standard test condition and different from the semiconductor behavior affecting output voltage, power, and durability. As a rule, temperature effect on crystalline silicon modules results in more significant decrease in voltage than minor increase in current so the power gain is negative overall. The temperature dependence of cells and modules was investigated previously; later, a review of correlation of efficiencies and powers for free-standing, BIPV, and photovoltaic-thermal modules was provided [1–3]. Hence, the effect on the output power is clear; under conditions of high irradiation and

insufficient cooling, a photovoltaic module can produce less power than suggested by its rated capacity.

Outdoors, the problem becomes even more complicated due to the fact that there are a number of interacting factors affecting the module temperature. The heat generation depends on irradiance, the lower thermal boundary is defined by ambient temperature, convection is affected by wind speed, and heat exchange from the rear side of a module to the ambient depends on mounting clearance. Consequently, a module cooling system that works well for certain values of irradiance, ambient temperature, wind speed, and mounting clearance may show poor results when changing the values of one or two parameters. This means that experimental data is needed for analysis of photovoltaic module cooling systems because although laboratory experiments and simulation models allow us to investigate mechanisms, outdoor measurements provide data about the cooling performance under conditions that correspond to actual application. That is why in the present study, the measured values outdoors are regarded as performance indicators for a whole cooling setup rather than just the demonstration of its efficiency.

Another complicating issue is related to the definition of a successful photovoltaic cooling design. Thermal designers pay attention to the extent of temperature reduction, while reliability engineers focus on temperature distribution, and power system specialists are interested in power gain and improvement of fill factor. All the effects are connected, yet their magnitudes do not coincide. Increased finning leads to reduced maximum temperature at the expense of added mass, whereas phase-change materials stabilize temperature variations during the daytime period with subsequent need for solidification during the night, and water devices increase heat removal efficiency but require energy for pumping and protection against leaks. That is why the evaluation of photovoltaic cooling designs should account for both thermal and electrical aspects. This is why multi-response interpretation is required in addition to ordinary before-and-after comparison.

This consideration is valid because thermal effects have more influence on reliability than on peak power. Increased degradation, solder-bond stresses, encapsulant darkening, backsheet embrittlement, and mismatch-related factors can depend on the thermal state of the module and its history of experiencing high and nonuniform temperatures. Large-scale studies and analysis of failure modes suggest that degradation occurs at different rates depending on climatic location, module type, choice of package, and stress profile. International reports about reliability confirm that temperature non-uniformities like hot spots can affect module lifetime adversely [4,5]. The recognition of this fact means that the goal of photovoltaic cooling goes beyond achieving the minimum average temperature of a module. Technically meaningful cooling system design must take into account not only the homogeneity of the process itself but also whether the electrical operating point becomes optimized in a thermally consistent manner.

Spatial temperature nonuniformity is especially significant for photovoltaic modules because of electrical, mechanical, and thermal interconnects between cells. A system with an adequate average temperature can suffer locally from thermal gradients that increase series resistance in strings, initiate the development of hot spots, or cause faster aging of specific portions of the cell matrix. Review articles on uniform cooling describe this problem as a matter of reliability and energy yield rather than heat transfer details alone [6,7]. This is especially true when considering the effect of heat sinks mounted on the rear surface of the module, for which a particular increase in area or convective ability can mean neglecting cooling in other zones. Outdoor photovoltaic heat sink therefore has to be evaluated not just by peak temperature reduction but also by the consistency of the resulting temperature field.

Many active, passive, and hybrid methods exist in the literature on photovoltaic cooling. Forced air, water, spray, and pumped liquid systems provide efficient cooling of a module; however, such systems need extra energy, wear components, have the danger of leakage, demand control system implementation, and require routine maintenance [8–10]. Combined PV/T collectors and hybrids featuring air or water collection utilize

extracted heat for further use and thus represent productive ways to cool photovoltaic modules, although they have limitations of hydraulic or pneumatic design and of heat usage scenarios [11–14]. Passive technologies attempt to reduce the cost by increasing efficiency of natural convection, conducting ability, phase change capacity, and radiation exchange without using any external sources of energy. Review papers dedicated to passive cooling, phase change material application, and global photovoltaic cooling emphasize that effective solutions have to balance efficiency gain against manufacturing simplicity and material expenses [15–18].

Finned aluminum heat sinks fit well in this class of devices. They are easy to make via extrusion, can be installed on a module's rear face without disturbing the frontal optical surface, and increase heat sink area. Efficiency of this system depends on the fin height, fin spacing, quantity, perforation, orientation, and its ability to promote simultaneous heat spreading and convective cooling. Research papers on heat sink behavior, container fins, planar reflector, wicking plate, and perforated fins illustrate the potential of fin design in affecting photovoltaic temperature and performance [19–23]. A finned module has a great promise as far as hardware is concerned, but requires an algorithm for evaluating its thermal and electrical effects together.

The recent finned and heat-sink investigations have shown that geometry cannot be simply characterized by increased surface area. Fins positioned close to one another might impede airflow, excessively tall fins would unnecessarily add mass without proportional heat transfer, perforations could help with convection at the expense of decreasing the conduction area, and multi-level fins would distribute the thermal path if appropriately aligned with the rear side geometry. Thus, the outdoor heat-sink problem involves both the choice of material and geometry optimization. While aluminum combines high thermal conductivity and feasibility of manufacture, the design would need to provide a clear enhancement in those parameters that matter for module performance.

The necessity of integrated assessment grew alongside the diversity of photovoltaic cooling research. Modern reviews stress the necessity to evaluate cooling approaches in terms of their systems-oriented practicability as well as effectiveness in reducing temperatures [24–27]. The same rationale applies to an integrated analysis within the confines of a compact two-module outdoor experiment. Any improvement in maximum power might turn out to negatively affect the spatial uniformity or protection of maximum power generation point. Alternatively, any drop in temperature levels might turn out to adversely affect both uniformity and power production. However, if the same cooling method manages to enhance all three criteria, the consistency of results would speak to its advantage.

Multiple criteria-based decision aids are relevant to the case of experimentally inconsistent results and finite number of physically distinguishable solutions. Grey Relational Analysis has proven to be an especially promising tool in such cases because it was designed for the situation when complete statistical information may not be available, but the notion of closeness to a target response sequence is still required [28,29]. The technique has already found applications in such areas as manufacturing, materials process engineering, renewable energy devices, and solar collectors thanks to its ability to normalize criteria and provide an overall grade based on their relative closeness to the target sequence. Rather than substituting physical reasoning, grey relational analysis helps to codify it.

This leads to the specific research question being posed by this study: when the performance of a rear truncated multi-level fin heat sink is analyzed using a grey relational analysis framework based on a coupled outdoor experiment comprising cooling efficiency, temperature uniformity, and operating-point parameters, does this approach show it to be a preferred photovoltaic solution and under what conditions regarding grey-relational settings. Rather than asking whether passive cooling is generally a viable solution, or whether fins reduce temperatures by definition, this question is focused on whether the available thermal-electrical evidence from the same experiment supports a decision in favor of the rear-fin heat sink. The point is that while most of the literature separately discusses cooling and power effects, the real-world decision-making challenge requires integration.

The contribution of the article is twofold in nature: firstly, it constructs a compact outdoor decision matrix for a rear finned photovoltaic monocrystalline module; secondly, it evaluates the impact of different parameter sets on the conclusions reached via the grey relational approach. This allows arriving at a straightforward and precise conclusion in response to the stated research question, rather than producing a broader and less targeted claim about photovoltaic cooling technologies. The manuscript thus makes full use of the available measured quantities, explicitly defines the criteria and assigns them weights and normalizes them into relational grades.

The formulation of the research question deliberately focuses on specifics rather than generalities. Neither global optimality of the selected fin geometry, nor substitution of the outdoor measurement results for long-term monitoring data are involved in the question being raised. The research question instead asks whether the thermal and electrical measurements, performed without suppressing the unfavorable I_{sc} response, select a finned solution. This is where the strongest evidentiary support can be achieved, leading to a complete manuscript of a defensible nature.

The outside configuration illustrated in Figure 1 demonstrates the controlled and paired nature of the investigation. Both the reference module and MLFHS module are exposed to an identical outdoor environment, and the rear fins visible on the rear side of the module provide the sole significant difference in hardware. Such evidence is vital to the reasoning in this manuscript because the subsequent results for thermal, electrical, and GRA analysis are analyzed in comparison to two matched photovoltaic systems instead of separate devices.

Figure 1. Outdoor module comparison.

2. Materials and Methods

The testing utilized two identical monocrystalline photovoltaic modules rated at 120 Wp. One module did not feature a rear-side cooling attachment and thus served as the reference configuration, whereas the second had a rear attachment of the MLFHS system. The numerical measurements employed in this study are from the outdoor experiment of Ahmad et al. [30]. The outdoor experiment is suitable for the present decision-making task since it provided data on thermal and electrical responses from modules of equal nominal power under outdoor conditions. This avoids the most common pitfall in comparing papers that differ by module rating, climate, testing protocol, or instrumentation type, which makes it challenging to determine whether observed performance differences stem solely from cooling technology.

Rear cooling hardware depicted in Figure 2 provides physical illustration of the cooling strategy implementation. The addition of multi-level fins made of aluminum increases

the convective area on the rear side of the module without any alterations to the optical front side surface of the solar cells module. As can be seen from the illustration below, the current cooling method is a thermal management experiment for a whole solar cell module rather than a new cell technology.

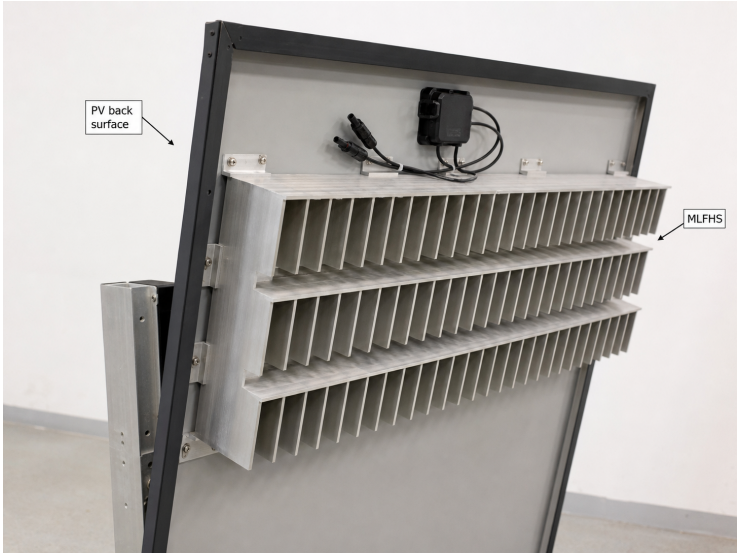

Figure 2. Rear heat-sink assembly.

The instrument configuration from Figure 3 bridges the outdoor environment with the decision matrix. While irradiance, temperature, and voltage-current measurements are present in the same experimental setup, it allows us to make an integrated evaluation based on those data. Therefore, the thermal criteria will be evaluated along with the electrical ones in operating-point space, not as separate readings collected in completely different settings.

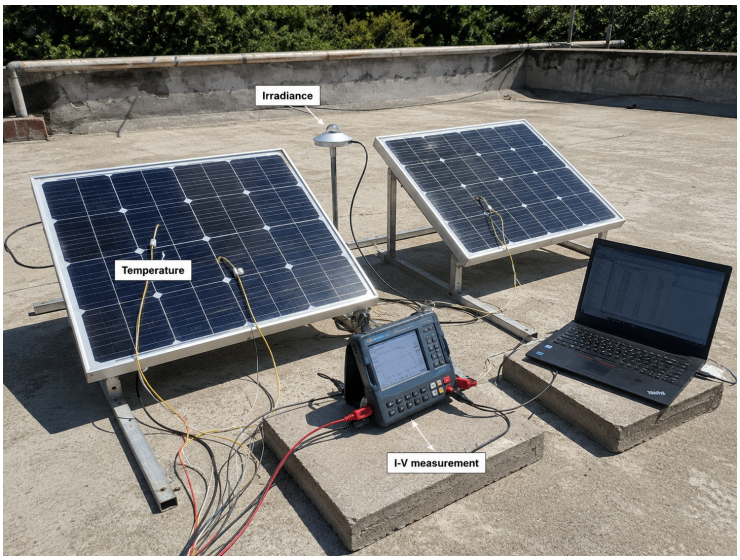

Figure 3. Outdoor instrumentation.

The nominal characteristics of the module are given in Table 1. They allow us to set the operating point scale physically and provide a reason to expect strong voltage dependence on temperature reduction. The power temperature coefficient is negative, the voltage temperature coefficient is negative, and the current temperature coefficient is very low and positive. Thus, we can assume that voltage and power would be most protected by

cooling, while the short-circuit current may be slightly dependent on it. The table therefore provides a physical basis for interpreting the measured outdoor electrical quantities rather than treating them as isolated numbers.

Table 1. Module properties.

Parameter	Value
Maximum power at standard test conditions, $P_{\max}$	120 Wp
Open-circuit voltage, V_{oc}	24.64 V
Short-circuit current, I_{sc}	6.21 A
Maximum-power voltage, V_{mp}	20.88 V
Maximum-power current, I_{mp}	5.75 A
Operating temperature range	−40 °C to 85 °C
Power temperature coefficient	−0.35 %/°C
Voltage temperature coefficient	−0.27 %/°C
Current temperature coefficient	0.05 %/°C

Based on the properties presented in Table 1, it can be seen that heat-sink effectiveness must not be primarily determined based on the short-circuit current. In particular, a negative voltage coefficient and a negative power coefficient imply that the effect of electrical cooling will manifest as increased open-circuit voltage, improved maximum power operation point, and higher power rectangle area. As for the current coefficient being only mildly positive, this implies that the small difference in I_{sc} could be impacted not only by temperature but also by other factors such as irradiance, optical condition, and/or measurement accuracy. This prediction is important since the outdoor record presented below reveals that one criterion favors the reference module while others prefer the finned module.

The decision matrix involves ten criteria, as indicated in Table 2. The first criterion pertains to the effectiveness of cooling which can be represented by the temperature drop produced by the fins. Three further criteria include temperature uniformity indices at 520 W/m^2, 940 W/m^2, and 640 W/m^2. These values of irradiance are used independently rather than being averaged together since they pertain to the ability of the heat sink in producing uniform spatial temperature drop depending on the outdoor solar radiation condition. The last six criteria are related to electrical parameters including I_{sc}, V_{oc}, I_{mp}, V_{mp}, power, and fill factor. Each criterion represents large-is-better.

Table 2. Decision matrix.

Criterion	Reference module	MLFHS module	Preference
Maximum cooling effectiveness, $\Delta T_{\max}$ (°C)	0.00	8.45	Larger
Temperature uniformity at 520 W/m^2	0.846	0.867	Larger
Temperature uniformity at 940 W/m^2	0.820	0.847	Larger
Temperature uniformity at 640 W/m^2	0.813	0.831	Larger
Short-circuit current, I_{sc} (A)	6.10	5.88	Larger
Open-circuit voltage, V_{oc} (V)	22.4	23.8	Larger
Current at maximum power, I_{mp} (A)	4.64	4.98	Larger
Voltage at maximum power, V_{mp} (V)	18.8	19.4	Larger
Maximum power, $P_{\max}$ (W)	87.23	96.61	Larger
Fill factor, FF	0.57	0.63	Larger

The trade-off presented in Table 2 is intentionally succinct but is neither simplistic nor idealized. The finned module excels in all four thermal criteria as well as in five out of six electrical criteria, although the latter still lacks in short-circuit current. Therefore, there really is a choice here, not an overwhelming win for one option and a loss of the other. Also, the criteria have quite distinct physical natures and units of measurement, making any simple averaging of their raw values physically meaningless. An adequate

multi-criteria method should take this into account while transforming each value into a unit-free criterion while maintaining its preference direction.

Selection of the criteria starts with the physical chain through which a rear heat sink affects the performance of a photovoltaic module. Effective cooling is a basic thermal property of fins, and the uniformity indices prevent the evaluation from favoring a solution that provides good thermal balance in one part of the module and leaves another part unbalanced. Electrical criteria check whether the thermal modification results in a corresponding change in electrical characteristics of the module. The V_{oc} value measures the preservation effect at the open-circuit operating point, while I_{mp}, V_{mp}, and $P_{\max}$ correspond to the point of highest efficiency in practical conditions. Finally, fill factor adds information regarding the nature of the I-V curve. Even though I_{sc} is not likely to benefit much from cooling, it has been chosen for the final list since ignoring the single unfavorable quantity would diminish the significance of the evaluation.

As for the distinction between measured data and decisions based on it, the latter cannot modify the physical data. In other words, normalization, coefficient generation, and grade computation take place after all physical measurements have been registered. This is an important academic practice, as it lets the reader analyze the physical data and understand where the grade comes from. In case of a dichotomous decision, the normalization produces a binary matrix of preferences. Although such a simple form might look disadvantageous, it actually does the opposite since it explicitly demonstrates which module is preferable according to which criterion.

Criterion normalization makes each criterion dimensionless in the range of $[0;1]$. Since all criteria in this case represent better-is-larger quantities, the normalized score for alternative i and criterion k is computed as

$$x_i^*(k) = \frac{x_i(k) - \min_i x_i(k)}{\max_i x_i(k) - \min_i x_i(k)}. \tag{1}$$

This equation assigns 1 to the better-performing module and 0 to the lower-performing module for each criterion because there are only two alternatives. The binary normalized result should not be mistaken for a loss of measurement detail. The physical magnitudes remain visible in Table 2; the normalized matrix records only the direction of superiority criterion by criterion so that the two module configurations can be compared in a common relational space.

The ideal reference sequence in the normalized space is $x_0^*(k) = 1$ for every criterion. The absolute deviation of each module from the ideal value is

$$\Delta_i(k) = |x_0^*(k) - x_i^*(k)|. \tag{2}$$

A module that achieves the better value for a criterion has zero deviation from the ideal sequence for that criterion. A module that does not achieve the better value has a deviation of one in this two-alternative case. This step is useful because it converts the decision from a question of raw magnitude into a question of closeness to the preferred response direction.

The grey relational coefficient is then obtained from

$$\xi_i(k) = \frac{\Delta_{\min} + \zeta\Delta_{\max}}{\Delta_i(k) + \zeta\Delta_{\max}}, \tag{3}$$

where ζ is the distinguishing coefficient and is usually chosen between 0 and 1. The base calculation uses $\zeta = 0.5$, which is a neutral choice commonly used in GRA applications. In the present two-alternative matrix, an ideal criterion receives a coefficient of 1.000 and a non-ideal criterion receives 0.333 when $\zeta = 0.5$. This transformation is intuitive: the best module for a given criterion is fully close to the ideal sequence, while the other module receives a penalized but nonzero relational coefficient.

The overall grey relational grade for alternative i is calculated as

$$\Gamma_i = \sum_{k=1}^{m} w_k \xi_i(k), \qquad \sum_{k=1}^{m} w_k = 1, \tag{4}$$

where $m = 10$ and w_k is the criterion weight. The equal-criterion case sets $w_k = 0.1$ for each criterion. Equal criterion weighting is applied as the first calculation, since it does not favor either the thermal or electrical block. Sensitivity calculations test for two potential sources of instability: whether the use of distinguishing coefficient changes the ranking, and whether the ranking is determined by the greater number of electrical criteria relative to thermal criteria.

Sensitivity analysis changes the value of ζ to 0.3, 0.5, and 0.7. Lowering the distinguishing coefficient heightens the contrast between ideal and non-ideal normalized criteria. Increasing the distinguishing coefficient decreases such contrast. Stability with respect to all three coefficients indicates that the ranking is not determined by the choice of arbitrary coefficient. Weighting cases compare four views: equal criterion weighting, thermal criteria only, electrical criteria only, and domain-balanced weighting. Under the domain-balanced approach, the total weight assigned to the four thermal criteria equals half of the total weight, and the total weight assigned to the six electrical criteria equals another half. This comparison is crucial, because it raises the question of whether the finned module continues to be preferred even if thermal and electrical evidence are weighted equally, rather than if ten criteria are treated independently.

The method itself is deliberately cautious. First, it does not produce a lot of calculated quantities in addition to the actual measurements. Second, it does not rely on the single average of temperatures as the only evidence in thermal block, as the question about the spatial uniformity of the field is part of the investigation. Thus, the method correctly describes the physics of the problem: the heat sink is expected to change rear surface heat dissipation, the thermal field influences voltage and power, and the decision matrix seeks whether these changes are significant enough to establish the preferred configuration of the outdoors experiment.

The four weighting cases are formulated with the interpretability in mind, not necessarily to provide the complete set. Equal criterion weighting asks the most straightforward question: What would happen if every measured response is assigned the same numerical value? Thermal criteria only ask whether the heat sink is preferred before considering any electrical data. Electrical criteria only, in turn, are asking the converse question, which also incorporates the penalty for open circuit current I_{sc}. Finally, the domain-balanced approach is the most cautious way to combine the results, because under no circumstances will the six electrical variables collectively outweigh the four thermal variables due to the sheer quantity.

All the calculations are reproducible from the values provided in the manuscript. When the distinguishing coefficient equals $\zeta = 0.5$, a normalized criterion whose deviation equals $\Delta_i(k) = 1$ will have $\Delta_{\min} = 0$, $\Delta_{\max} = 1$, and hence $\xi_i(k) = 0.333$. A normalized criterion with no deviations ($\Delta_i(k) = 0$), on the other hand, will yield $\xi_i(k) = 1.000$. The grade for finned module will therefore equal the average of nine ideal $\xi_i(k)$ and one non-ideal $\xi_i(k)$, whereas the grade for reference case will equal the average of one ideal $\xi_i(k)$ and nine non-ideal $\xi_i(k)$.

3. Results and Discussion

Thermal data provides the first indication of the rear multi-level fin heat sink affecting module performance significantly. The maximum possible cooling effect of 8.45 °C is considerable compared to the power temperature coefficient of the module which is $-0.35\,\%/^{\circ}\mathrm{C}$. By using a coefficient based approximation, 8.45 °C could be estimated to translate to a power-preservation possibility of about 2.96% for the module if all other conditions remain constant. The measured power difference is higher than this coefficient based estimation; meaning that there is a factor beyond temperature variation affecting

the benefit. Improved voltages, maximum power point variations, and heat distribution are all factors that help determine the resulting outdoor power of modules. This finding is in agreement with existing photovoltaic literature on cooling where temperature reduction alone cannot explain power output without considering other parameters like current–voltage curves and field conditions [31,32].

Uniformity index results reveal the lack of locality in the cooling effects caused by the heat sink. For the three different irradiances of 520 W/m^2, 940 W/m^2, and 640 W/m^2, the uniformity index value rises to 0.867, 0.847, and 0.831 respectively. Absolute improvements of 0.021, 0.027, and 0.018 are achieved alongside respective percentages of 2.48%, 3.29%, and 2.21%. While these numerical values are relatively insignificant, they carry importance due to the close proximity of index values to 1. Consistency of the improvement in the index for all three irradiances suggests that the heat sink enhances heat extraction uniformity for all favorable conditions rather than focusing on one. This result is particularly relevant from a reliability perspective given the emphasis on the significance of uniform heat extraction in existing literature [5,7].

The thermal results from Figure 4 should be taken in combination as a result of heat rejection and heat distribution. The cooling effect metric is simply a drop in temperature level, and the three uniformity results are spatial improvements under three irradiance conditions. An increase in heat rejection but loss of uniformity using the back fin array might make sense for indoor modules but not for outdoor ones as it could just transfer the problem instead of solving it. In this case, the same array accomplishes heat rejection and uniformity improvement. Therefore, a passive cooling effect can be argued, in which the multi-level structure seems to enhance the heat rejection channels without creating obvious uniformity penalty.

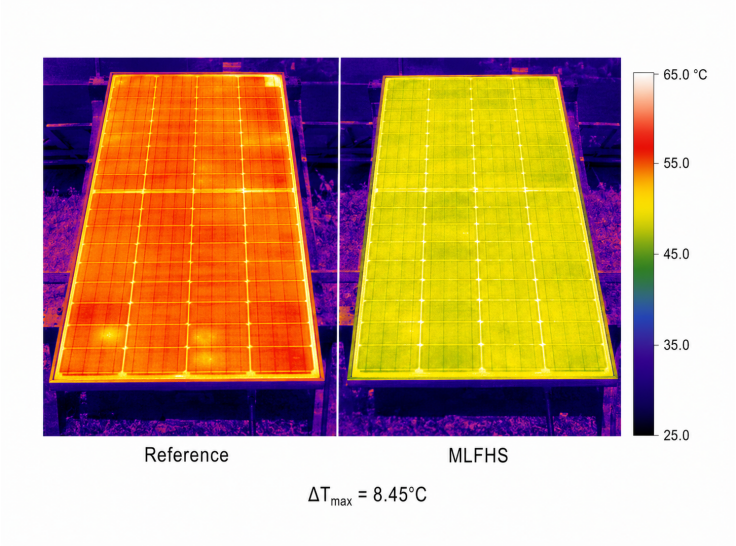

Figure 4. Thermal field comparison.

This aspect of heat rejection versus electrical benefit becomes especially important in explaining the benefits of the configuration in light of mixed readership. Heat transfer engineers will focus on the 8.45 °C reduction and uniformity improvement, while photovoltaics system designers may want to see the maximum power point and the fill factor instead. However, the dataset offers a solution to reconcile the two viewpoints. One may understand the reason why the voltage increases based on heat transfer, whereas the other may explain the reason why the thermal action has any practical meaning in terms of electricity production.

It is also worth comparing the magnitude of the cooling action with its passive nature. An active device can possibly accomplish greater temperature reduction, but the net electrical value should still be adjusted to account for the energy consumed. A rear metal

heat sink has no such cost because its operation consumes no power; thus, the power gain is not compensated by auxiliary power needs. It does not mean that there are no engineering challenges, since material and structural issues exist. Nonetheless, the comparison between the two aspects becomes much easier: the power gain is due to the geometric action of the rear array without any electrical effort.

Finally, it is noteworthy that the uniformity gain at 940 W/m^2 is the largest among all three values. The irradiance dependency also plays a role in interpreting this data set. At that irradiance level, the non-finned module shows the smallest uniformity, 0.820, whereas the fin array improves the index up to 0.847. Thus, the greatest improvement of uniformity happens at high irradiance, during which thermal gradients become increasingly important due to high heat generation rates.

From the electric measurements, it can be concluded that the thermal optimization has reached the practical working point. The open circuit voltage increases from 22.4 V to 23.8 V, or a voltage increase of 1.4 V (~ 6.25%). The maximum power voltage increases from 18.8 V to 19.4 V, while the maximum power current increases from 4.64 A to 4.98 A. As maximum power equals the multiplication of current and voltage in maximum power, the combined enhancement of I_{mp} and V_{mp} is thus more significant than an individual increase. The $P_{\max}$ measured increased from 87.23 W to 96.61 W, with an absolute gain of 9.38 W. Compared to the benchmark, the gain in percentage terms amounts to around 10.75% from the table values. It is also noticed that the fill factor rises to 0.63 from 0.57, which suggests that the finned module exhibits a better current-voltage curve profile when compared with its counterpart in the tested outdoor environment.

The reverse flow of the short-circuit current decreases from 6.10 A for the reference module to 5.88 A for the finned module. However, this single deviation is insufficient to reject the electrical explanation. Short-circuit current is not so sensitive to temperature compared to voltage in crystalline-silicon solar modules, and the nominal coefficients for a module in Table 1 have a very low value of the positive current coefficient compared to the negative values of the voltage and power coefficients. A slight reduction in the short-circuit current can be observed simultaneously with an increase in the maximum power if the voltage and maximum power output conditions improve enough. That is precisely what is happening here. The short-circuit current for the finned module has decreased by 0.22 A, while the open-circuit voltage increased by 1.4 V.

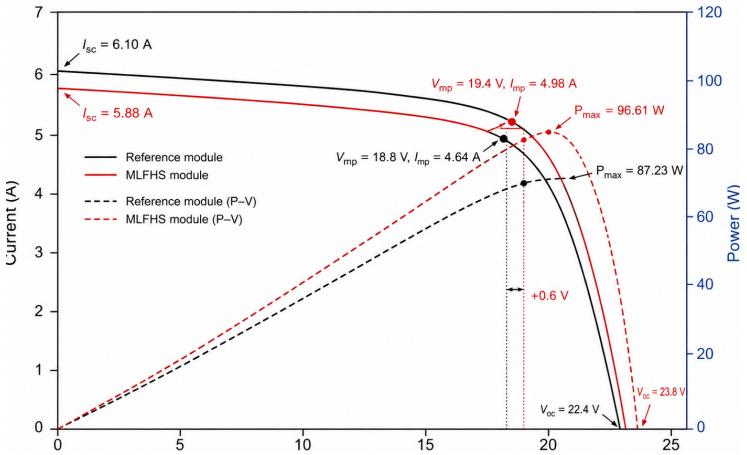

Figure 5. Operating-point response.

It becomes clear from the electrical data in Figure 5 that the focus on maximum-power operation is justified by the nature of the comparison. While the reference module has an advantage in terms of I_{sc} alone, the finned module dominates all voltage and power metrics. This agrees with our physical expectations. We expect that cooling a crystalline silicon-based solar cell should be more effective at maintaining high voltage and power levels than modifying short-circuit current [1,3]. In other words, we have not obtained an

artifact due to some statistical fluke. This means that we should not abandon the heatsink simply because a particular current measure is reduced. We should consider it because power performance improves significantly.

Normalization helps with better understanding the relative values of the raw criteria. The normalized criteria in Table 3 show that the finned module wins nine out of ten criteria against the reference module. The sole criterion with the higher rating for the reference module is short-circuit current. This fact becomes important when we understand that the grey relational grade is nothing more than a sum of the distances from ideal criterion rankings. The dominance of one module across most criteria makes it likely that it will dominate the overall GRA ranking, unless we assign too much weight to the single opposing criterion.

Table 3. Normalized matrix.

Criterion	Reference module	MLFHS module
Maximum cooling effectiveness, $\Delta T_{\max}$	0	1
Temperature uniformity at 520 W/m^2	0	1
Temperature uniformity at 940 W/m^2	0	1
Temperature uniformity at 640 W/m^2	0	1
Short-circuit current, I_{sc}	1	0
Open-circuit voltage, V_{oc}	0	1
Current at maximum power, I_{mp}	0	1
Voltage at maximum power, V_{mp}	0	1
Maximum power, $P_{\max}$	0	1
Fill factor, FF	0	1

As is clear from the normalized values presented in Table 3, the considered conflict does not represent the case of balanced opposition of two equivalent alternatives. It represents the case of dominance with a single exception that can be explained in physical terms. Thermal block is completely supportive for the finned module, while electrical block is supportive for the finned module in five out of six criteria. The only exception in terms of value is associated with the current parameter, which, in contrast to voltage and power, is assumed to be weakly sensitive to heat removal. However, such a criterion structure still implies the leading role of finned module.

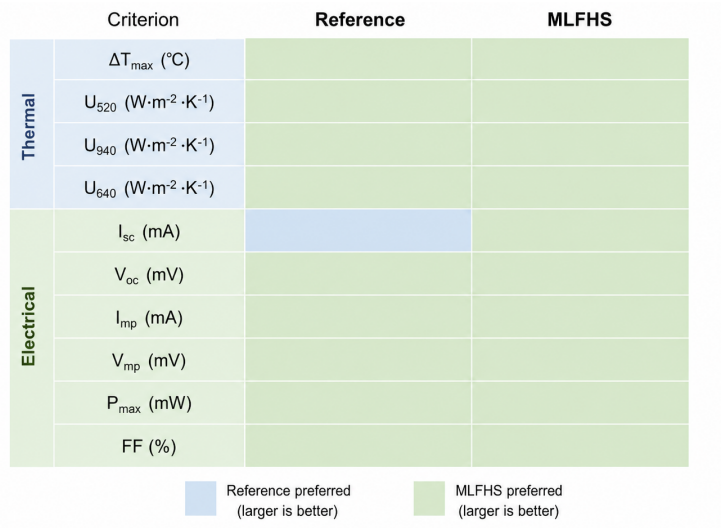

Figure 6. Criterion dominance matrix.

The criterion dominance matrix presented in Figure 6 emphasizes the asymmetry of the conclusion. The finned module appears to be preferable to the other in most of the

examined criteria. In a less definite scenario, one would expect a constant exchange of superiority between the thermal and electrical criteria groups, which would result in a subjective sensitivity of the ranking process to weight factors. In the present case, one can see a completely different picture: the only opposing factor is the criterion of current, whereas the thermal and maximum power performance criteria form a dominating decision direction. That is the reason for a clear distance between the grey relational grades of the modules.

The grey relational coefficients provided in Table 4 can be calculated based on the normalized criterion matrix using $\zeta = 0.5$. The reference module is characterized by one ideal and nine non-ideal coefficients, while the finned module gets nine ideal and one non-ideal coefficient. Under the same weights for both sets of factors, the reference grade equals 0.400 while the finned-module grade is 0.933. As the grade difference equals 0.533, it cannot be seen as a marginal preference. It indicates that the finned module is much closer to the ideal multi-response sequence across the defined outdoor criteria.

Table 4. GRA coefficients.

Criterion	Reference module	MLFHS module
Maximum cooling effectiveness, $\Delta T_{\max}$	0.333	1.000
Temperature uniformity at $520\,\mathrm{W/m^2}$	0.333	1.000
Temperature uniformity at $940\,\mathrm{W/m^2}$	0.333	1.000
Temperature uniformity at $640\,\mathrm{W/m^2}$	0.333	1.000
Short-circuit current, I_{sc}	1.000	0.333
Open-circuit voltage, V_{oc}	0.333	1.000
Current at maximum power, I_{mp}	0.333	1.000
Voltage at maximum power, V_{mp}	0.333	1.000
Maximum power, $P_{\max}$	0.333	1.000
Fill factor, FF	0.333	1.000
Grey relational grade, Γ_i	**0.400**	**0.933**

Furthermore, the coefficient matrix itself is of some additional interpretive interest in terms of what it reveals about the preference origin. There are four coefficients that can be considered ideal according to thermal variables and five ideal coefficients according to electrical variables. In other words, the choice of the heat sink does not occur simply due to the presence of several electrical variables or due to the fact that cooling efficiency was high in the analysis. The decision is thus based on both sets of criteria, which is very valuable in terms of passive cooling. The idea is that a solution that helps improve temperature but does not affect the maximum power output point is likely to have a lower level of practical value. However, the finned module is shown to provide results that align well with the heat transfer criterion and the criterion of electrical performance.

It might be useful to look at the grade separation differently. With equal weights applied, the MLFHS module receives just one fewer coefficient-level result compared to the ideal case when the vector is full of ones, while the reference module receives nine less coefficients. In addition, this one coefficient-level result happens to be linked with the criterion that is the least related to the process of thermal voltage formation. Overall, this is why such a comparison becomes more meaningful than simple grades because, as noted earlier, 0.933 is indeed higher than 0.400, but it comes from the same physical patterns as expected from reduced temperature and enhanced heat transfer.

The coefficient matrix might prove valuable to the future work in photovoltaics because of the way it provides proof of design. Experimental papers tend to provide separate sections for describing cooling and increased electricity output, and the readers must make the inference themselves. In other words, they do not see the direct relationship between the two. However, it is provided here, which will make design transfer easier.

Figure 7 provides auditable evidence to support the GRA ranking since the finned module has the ideal coefficient for each criterion, except for I_{sc}. In contrast, the reference

module has the ideal coefficient only for I_{sc}. This feature is one of the advantages of GRA for small datasets from outdoor engineering environments. The procedure does not hide the trade-offs; the trade-offs are shown explicitly even though GRA offers a single grade. A reader can confirm or refute the ranking based on the criteria, rather than accepting or questioning the grade as a number.

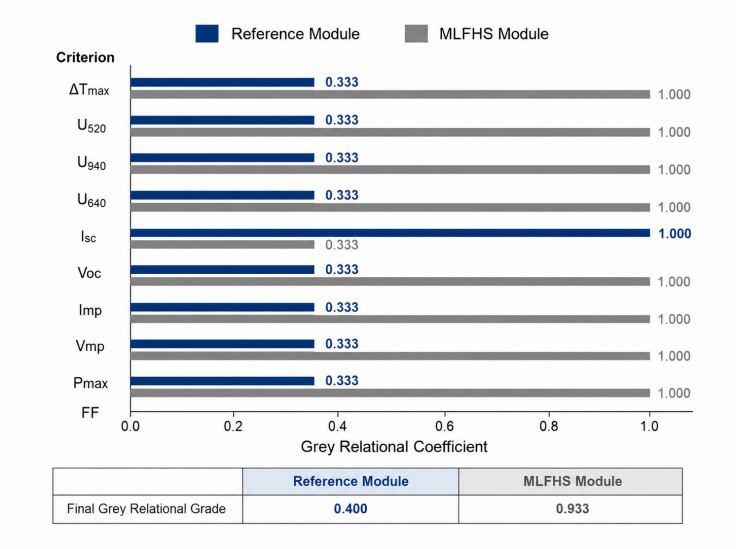

Figure 7. GRA coefficient profile.

The test of sensitivity regarding the distinguishing-coefficient criterion examines whether the separation of the two modules depends on the choice of the contrast parameter. The figures in Table 5 demonstrate that the finned module remains preferable with $\zeta = 0.3$, $\zeta = 0.5$, and $\zeta = 0.7$. When the contrast parameter decreases, the penalties increase, resulting in lower grades for both modules with non-ideal coefficients. At higher contrast parameters, the penalty is reduced and higher grades result. Importantly, the order of the modules does not change.

Table 5. Coefficient sensitivity.

ζ	Reference module	MLFHS module	Preferred module
0.3	0.308	0.923	MLFHS
0.5	0.400	0.933	MLFHS
0.7	0.471	0.941	MLFHS

The sensitivity values in Table 5 indicate that the ranking is structural rather than tuned. A decision that reversed when ζ changed modestly would be difficult to defend because the contrast parameter would be controlling the conclusion. Here, the physical dominance pattern controls the conclusion. The finned module leads because it is ideal in nine of ten criteria, not because the grey-relational coefficient has been selected to magnify a small advantage. This robustness strengthens the answer to the research question because it shows that the preference survives reasonable variation in the relational contrast.

The robustness matrix presented in Figure 8 also offers insight into the problem. While both grades increase as ζ increases due to the lower impact of the non-ideal coefficient, their separation is still large. This can be explained in view of the dominance of one alternative on such a robustness matrix. Practically speaking, the engineer can use a highly discriminating or low-discriminating coefficient and still get the same cooling configuration as an optimal one. Thus, the heat sink advantage appears to be robust even to the setting of the method.

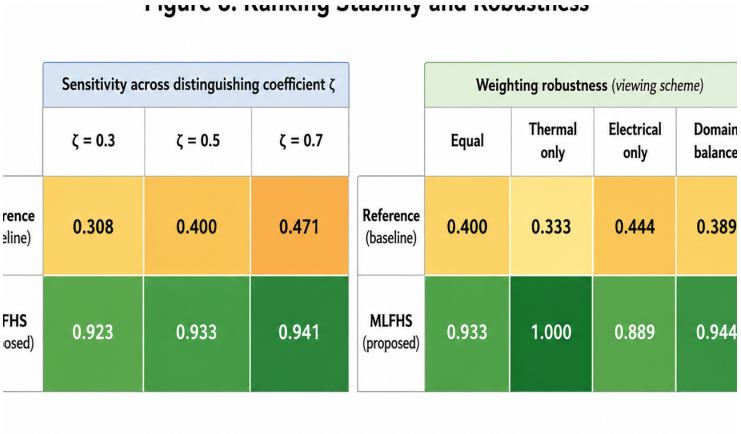

Figure 8. Robustness matrix.

Another robustness test is offered by the results of the weight analysis given in Table 6. When equally-weighted criteria are used, the finned module is awarded a grade of 0.933 versus 0.400 for the reference module. In case of the thermal perspective only, the grades for the modules would be 1.000 versus 0.333 as all thermal criteria prefer the heat sink. For the electrical perspective, which is based on six criteria including I_{sc}, the grades are 0.889 and 0.444 respectively. Finally, with equal weights applied to thermal and electrical blocks, the grades become 0.944 and 0.389 correspondingly.

Table 6. Weighting robustness.

Weighting view	Reference module	MLFHS module	Preferred module
Equal criterion weights	0.400	0.933	MLFHS
Thermal criteria only	0.333	1.000	MLFHS
Electrical criteria only	0.444	0.889	MLFHS
Thermal–electrical domain balance	0.389	0.944	MLFHS

The weighting results are essential since they address a potential criticism that could be leveled against the ten-criterion matrix. There are six electrical and four thermal criteria, so it would make sense to argue that equal criterion weighting results in more influence from electrical behavior. The domain-balanced analysis solves the problem, as thermal and electrical evidence receive equally high domain influence. Moreover, the order does not change. The electrical only ranking also remains advantageous despite the reference module winning the I_{sc} criterion. Thus, electrical value of the heat sink is independent of thermal parameters and appears in the operating point current-voltage and maximum power generation measurements.

Domain-balancing is particularly helpful when writing a complete manuscript, as it splits evidence and presentation decisions into separate sections. Specifically, the thermal block includes one criterion for effectiveness of cooling and three criteria for temperature uniformity of the heat sink surface. The electrical block involves six circuit quantity measures. While some readers might want to place more weight on thermal performance and others more weight on the power electronics aspect, the preference is not reflected in rankings, which stay unchanged throughout the considered views. In other words, the heat sink selection is based on a thermal measure, on an electrical measure, and on both types of criteria.

Small-scale datasets are particularly appropriate for robustness checks, as they do not allow the use of statistical testing methods requiring larger samples. Two alternative configurations are physical module designs, rather than draws from a large dataset, so the clarity and consistency of criteria and sensitivity of the decision rule play an even greater role in the assessment of the optimal setup. Manuscript authors treat robustness in terms of stability of the preferred module under different contrasts and weights. Thus, consistent ranking implies higher reliability of the integrated conclusion.

In turn, it can be explained with reference to the physics of crystalline silicon-based solar modules operation. Cooling decreases cell temperatures, while low temperatures yield increased voltage from the solar cell. Since maximum power is governed by both the current and the voltage in the operation point, a voltage preserving approach to reducing thermal load might lead to higher $P_{\max}$ despite unchanged I_{sc}. The fill factor improvement indicates that the rear-finned design also contributes to better shape of the characteristic. In practical outdoor terms, this means that the rear-finned module looks cooler, but also generates more power at the relevant operating point. That is what distinguishes an effective cooling mechanism from an ineffective performance enhancement tool.

In this context, uniformity index analysis provides additional supporting evidence. One potential issue with passive cooling systems might be the inability to ensure homogeneous spreading of heat through the material. According to results presented in the table above, however, the MLFHS system achieves this goal better than a plain surface in all irradiance levels tested. The largest improvement is observed for 940 $\mathrm{W/m^2}$, when the temperature-related effects might be stronger. This feature is positive since it is just under high irradiance that thermal gradients, heating up and consequent voltage drop have the biggest effect. The ability to operate better with increasing irradiance is a significant feature in outdoor operation conditions.

Finally, the obtained findings fit well into the general pattern of advantages and disadvantages for passive cooling vs. active. As was noted above, the latter are capable of achieving higher cooling effect, but the efficiency is affected by auxiliary energy expenditure. Passive systems based on the use of rear fins, however, do not require any pumping power, so there is no need to calculate the auxiliary losses. Nevertheless, this does not imply that passive fins always yield better results than active systems. Increased mass, weight, cost, wind influence and attachment difficulties should also be taken into consideration. Nevertheless, according to results obtained in this study, MLFHS provides a good balance between heat dissipation and power output without any energy losses associated with auxiliary equipment. That makes passive cooling an interesting direction in PV-thermoelectric systems [33,34].

It also demonstrates the correct way to report a compact outdoor experiment. Two modules are not sufficient to support conclusions for every climate and for every kind of module technology, but they are sufficient to support a rigorous internal comparison if the modules are identical and the criteria are explained correctly. The current measurement matrix preserves that rigorous internal comparison. It does not aggregate all variables to a single number that is not explained. And it does not give every electrical number equal weight without explaining the choice. In addition to the GRA, the raw measurement matrix, normalized matrix, coefficient table, and sensitivity analysis are provided. This kind of reporting is useful for photovoltaics because it helps a reader identify whether the GRA supports the decision in terms of physics.

A few limitations are important here. As explained earlier, the current comparison relies on one module rating, one heat-sink geometry, and limited outdoor measurement data. Seasonality, wind direction, soiling, rear clearance, module mounting, corrosion, fatigue, and total system lifetime cost are issues that cannot be addressed with the present matrix alone. Outdoor testing over many years will be required to determine whether the thermal uniformity improvement leads to less degradation or to lower failure rate. Different modules can react differently due to differing temperature coefficients. None of these considerations reduces the significance of the current decision; they merely highlight the next experimental level to address.

A future outdoor test could also benefit from the current decision matrix. The missing piece is not an aggregated score but long-term time-resolved data linking the factors such as wind speed, solar radiation, temperature of the rear surface, and maximum-power tracking algorithm. This kind of test would help to verify whether the same criteria dominance exists in the morning warm-up phase, mid-day thermal-loading phase, and afternoon cooling phase. Additionally, it would enable researchers to separate the effect of heat-sink

geometry from the transient environmental factors. The present result provides justification for conducting this test, since the matrix already exhibits thermal-electrical coherence.

The paper also explains why the comparison of outdoor values against STC rating must be done carefully. Since both outdoor modules are under the nominal value of 120 Wp, it is natural to expect it, given that outdoor conditions such as cell temperature, irradiance variations, and module mounting conditions are different from those used in the STC testing procedure. The correct comparison is not between each outdoor measurement and the rating number; the comparison is between the reference and finned modules within the same outdoor measurement record. On that basis, the value 96.61 W of the finned module is not only lower than STC, it is 9.38 W greater than that of the reference module within the outdoor environment.

A further improvement would come in the form of heat-sink geometry-family comparison. The rectangular-fins heat-sink, the perforated fins heat-sink, the multi-level fin heat-sink, and the reference heat-sink can be compared according to the same criterion set. The two-module comparison has already established that the MLFHS configuration performs better than the unmodified reference module in the current data record. The geometry-family comparison will help to determine whether the multi-level geometry is a critical factor for performance improvement or not. From the manufacturing standpoint, the former is less attractive, since it is more complicated to manufacture.

The more general lesson is that passive photovoltaic cooling systems must demonstrate variable coherency for a practical application. An improvement of only one variable produces a narrow and possibly meaningless result. The present MLFHS module exhibits a more coherent picture because several variables improve at once: the temperature level, thermal uniformity, voltage, maximum power current, maximum power voltage, maximum power itself, and fill factor all change positively. One deviation, the short-circuit current, can be physically understood and is insignificant compared to the other changes. Hence, the answer to the research question is not statistical but physical: the finned module must be preferred because its thermal improvements correlate well with temperature-sensitive electrical quantities.

From a design standpoint, the results suggest that rear heat sinks should be treated as thermal spreaders rather than as additional fin area. The effectiveness of the multi-level arrangement is supported by the facts that both temperature level and thermal uniformity improved. If the geometry would increase heat transfer only in specific regions of the module back, the thermal uniformity indices would not shift uniformly in a desirable direction. Therefore, the multi-level arrangement seems effective at increasing thermal conductivity of the rear surface and at maintaining voltage benefits of decreased temperature operation. This is generally consistent with the conclusion that passive heat sinks need geometrical optimization and not surface area addition [20,23].

The economic significance of the result cannot be determined from the given numerical information. However, the presented matrix can provide some initial guidance. A 9.38 W increase in maximum power of a 120 Wp module is significant at the module scale. Depending on the material price, the climate, mounting design, and estimated service lifetime, the improvement might or might not justify the added material costs and installation efforts. Nevertheless, the power gain was achieved without requiring auxiliary energy source. In addition, uniformity has been improved, which could make the geometry attractive beyond its immediate effect. If future lifetime test verifies improved durability or hot-spot risk reduction, the uniformity improvement will become even more appealing.

4. Conclusion

The research question was posed about whether the fin-based multi-level heat-sink module is still optimal outdoor PV module compared to the reference design under combined cooling, temperature uniformity, and operating point metrics criteria. The answer in favor of the heat-sink module can be obtained for the measured data in the 120 Wp monocrystalline test case. Cooling effectiveness is increased by 8.45 °C on the fin-based

module. It also helps improve the temperature-uniformity index at power densities of 520 W/m^2, 940 W/m^2, and 640 W/m^2. The heat-sink module positively affects electrical parameters that ensure proper operating conditions: V_{oc} is increased from 22.4 V to 23.8 V; I_{mp} increased from 4.64 A to 4.98 A; V_{mp} increased from 18.8 V to 19.4 V; $P_{\max}$ increased from 87.23 W to 96.61 W; fill factor increased from 0.57 to 0.63. In addition to all of the above, the criterion I_{sc} is the only parameter for which a higher value is achieved on the reference module.

Applying the Grey Relational Analysis tool converts the findings into quantitative measures of superiority. The finned module acquires a grey relational grade of 0.933 with equal criterion weights and $\zeta = 0.5$. Meanwhile, the reference module receives a lower grade of 0.400. Further, the ranks do not change when ζ is changed in the range of 0.3 to 0.7. When the criteria are analyzed separately according to the equal-criterion weightings, only thermal, only electrical, and thermal-electrical domain-balanced sets of criteria give the same ranks. Thus, the result cannot be explained by the choice of the criterion weighting set. Rather, it is determined by the matrix structure where the fin module outperforms the reference module on nine out of ten criteria.

In practice, the conclusion made here is narrow rather than broad. One should not conclude that fin modules are more preferable because any cooling solution is better than no cooling from the principle standpoint. The measured data show a consistent performance advantage of the heat-sink module on cooling effectiveness, temperature uniformity, and electrical performance. The rear fin geometry appears to improve both the thermal and electrical characteristics in an integrated way. The future studies may focus on different seasons, wind regimes, fin geometries, lifecycle cost, mechanical strength, and longevity issues, but for the given experimental conditions, the conclusion is clear: the MLFHS module is the preferred outdoor photovoltaic module.

References

[1] Radziemska, E. (2003). The effect of temperature on the power drop in crystalline silicon solar cells. Renewable energy, 28(1), 1-12.

[2] Skoplaki, E., & Palyvos, J. A. (2009). On the temperature dependence of photovoltaic module electrical performance: A review of efficiency/power correlations. Solar energy, 83(5), 614-624.

[3] Dubey, S., Sarvaiya, J. N., & Seshadri, B. (2013). Temperature dependent photovoltaic (PV) efficiency and its effect on PV production in the world–a review. Energy procedia, 33, 311-321.

[4] Jordan, D. C., & Kurtz, S. R. (2013). Photovoltaic degradation rates—an analytical review. Progress in photovoltaics: Research and Applications, 21(1), 12-29.

[5] Köntges, M., Kurtz, S., Packard, C. E., Jahn, U., Berger, K. A., Kato, K., ... & Friesen, G. (2014). Review of failures of photovoltaic modules.

[6] Simon, M.,& Meyer, E. L. (2010). Detection and analysis of hot-spot formation in solar cells. Solar energy materials and solar cells, 94(2), 106-113.

[7] Bahaidarah, H. M., Baloch, A. A., & Gandhidasan, P. (2016). Uniform cooling of photovoltaic panels: A review. Renewable and Sustainable Energy Reviews, 57, 1520-1544.

[8] Krauter, S. (2004). Increased electrical yield via water flow over the front of photovoltaic panels. Solar energy materials and solar cells, 82(1-2), 131-137.

[9] Teo, H. G., Lee, P. S., & Hawlader, M. N. A. (2012). An active cooling system for photovoltaic modules. applied energy, 90(1), 309-315.

[10] Royne, A., Dey, C. J., & Mills, D. R. (2005). Cooling of photovoltaic cells under concentrated illumination: a critical review. Solar energy materials and solar cells, 86(4), 451-483.

[11] Charalambous, P. G., Maidment, G. G., Kalogirou, S. A., & Yiakoumetti, K. (2007). Photovoltaic thermal (PV/T) collectors: A review. Applied thermal engineering, 27(2-3), 275-286.

[12] Tonui, J. K., & Tripanagnostopoulos, Y. (2007). Improved PV/T solar collectors with heat extraction by forced or natural air circulation. Renewable energy, 32(4), 623-637.

[13] Tonui, J. K., & Tripanagnostopoulos, Y. (2007). Air-cooled PV/T solar collectors with low cost performance improvements. Solar energy, 81(4), 498-511.

[14] Zondag, H. A. (2008). Flat-plate PV-Thermal collectors and systems: A review. Renewable and Sustainable Energy Reviews, 12(4), 891-959.

[15] Hasan, M. A., & Sumathy, K. (2010). Photovoltaic thermal module concepts and their performance analysis: A review. Renewable and sustainable energy reviews, 14(7), 1845-1859.

[16] Hasanuzzaman, M., Malek, A. A., Islam, M. M., Pandey, A. K., & Rahim, N. A. (2016). Global advancement of cooling technologies for PV systems: A review. Solar Energy, 137, 25-45.

[17] Elbreki, A. M., Alghoul, M. A., Sopian, K., & Hussein, T. (2017). Towards adopting passive heat dissipation approaches for temperature regulation of PV module as a sustainable solution. Renewable and Sustainable Energy Reviews, 69, 961-1017.

[18] Siecker, J., Kusakana, K., & Numbi, E. B. (2017). A review of solar photovoltaic systems cooling technologies. Renewable and Sustainable Energy Reviews, 79, 192-203.

[19] Wongwuttanasatian, T., Sarikarin, T., & Suksri, A. J. S. E. (2020). Performance enhancement of a photovoltaic module by passive cooling using phase change material in a finned container heat sink. Solar Energy, 195, 47-53.

[20] Arifin, Z., Suyitno, S., Tjahjana, D. D. D. P., Juwana, W. E., Putra, M. R. A., & Prabowo, A. R. (2020). The effect of heat sink properties on solar cell cooling systems. Applied Sciences, 10(21), 7919.

[21] Parkunam, N., Pandiyan, L., Navaneethakrishnan, G., Arul, S., & Vijayan, V. (2020). Experimental analysis on passive cooling of flat photovoltaic panel with heat sink and wick structure. Energy Sources Part A-recovery Utilization and Environmental Effects, 42(6), 653-663.

[22] Elbreki, A. M., Muftah, A. F., Sopian, K., Jarimi, H., Fazlizan, A., & Ibrahim, A. (2021). Experimental and economic analysis of passive cooling PV module using fins and planar reflector. Case Studies in Thermal Engineering, 23, 100801.

[23] Hudișteanu, S. V., Țurcanu, F. E., Chereches, N. C., Popovici, C. G., Verdeș, M., & Huditeanu, I. (2021). Enhancement of PV panel power production by passive cooling using heat sinks with perforated fins. Applied Sciences, 11(23), 11323.

[24] Sharaf, M., Yousef, M. S., & Huzayyin, A. S. (2022). Review of cooling techniques used to enhance the efficiency of photovoltaic power systems. Environmental science and pollution research, 29(18), 26131-26159.

[25] Herrando, M., & Ramos, A. (2022). Photovoltaic-thermal (PV-T) systems for combined cooling, heating and power in buildings: a review. Energies, 15(9), 3021.

[26] Sato, D., & Yamada, N. (2019). Review of photovoltaic module cooling methods and performance evaluation of the radiative cooling method. Renewable and Sustainable Energy Reviews, 104, 151-166.

[27] Chandel, S. S., & Agarwal, T. (2017). Review of cooling techniques using phase change materials for enhancing efficiency of photovoltaic power systems. Renewable and Sustainable Energy Reviews, 73, 1342-1351.

[28] Julong, D. (1989). Introduction to grey system theory. The Journal of grey system, 1(1), 1-24.

[29] Liu, S., Forrest, J., & Yang, Y. (2011, September). A brief introduction to grey systems theory. In Proceedings of 2011 IEEE International Conference on Grey Systems and Intelligent Services (pp. 1-9). IEEE.

[30] Ahmad, E. Z., Sopian, K., Fazlizan, A., Jarimi, H., & Ibrahim, A. (2022). Outdoor performance evaluation of a novel photovoltaic heat sinks to enhance power conversion efficiency and temperature uniformity. Case Studies in Thermal Engineering, 31, 101811.

[31] Tiwari, G. N., Mishra, R. K., & Solanki, S. C. (2011). Photovoltaic modules and their applications: a review on thermal modelling. Applied energy, 88(7), 2287-2304.

[32] Sun, X., Silverman, T. J., Zhou, Z., Khan, M. R., Bermel, P., & Alam, M. A. (2017). Optics-based approach to thermal management of photovoltaics: selective-spectral and radiative cooling. IEEE Journal of Photovoltaics, 7(2), 566-574.

[33] Makki, A., Omer, S., & Sabir, H. (2015). Advancements in hybrid photovoltaic systems for enhanced solar cells performance. Renewable and sustainable energy reviews, 41, 658-684.

[34] Jia, Y., Alva, G., & Fang, G. (2019). Development and applications of photovoltaic–thermal systems: A review. Renewable and Sustainable Energy Reviews, 102, 249-265.